

Chapter 5

Optical diffraction in chiral smectic C liquid crystals : Theoretical study

5.1 Introduction

In chapter 4 we saw that our experimental results could not be explained by RN theory. In RN theory, the approximations that the amplitude of the phase modulation of the corrugated wavefront is much less compared to its wavelength allows us to treat the phase modulation and the diffraction processes separately. In this procedure we assume that, light beam travels along a straight line inside the medium and picks up the local phase during its passage. But in our experiments, due to the large thicknesses of the cells and the high birefringence of the sample used, the internal diffractions inside the grating are quite significant. Under this situation the phase modulation and the diffraction processes have to be treated simultaneously inside the grating. To incorporate these effects we use a rigorous coupled wave analysis for anisotropic dielectric grating following Rokushima and Yamakita (RY) [1]. In this approach we consider that there is more than one plane wavefront propagating inside the grating. The theory also takes care of the multiple reflections arising at the interfaces of liquid crystal and the bounding isotropic media. In this chapter we develop the RY theory for our problem and discuss the experimental results of chapter 4 in the context of this theory.

5.2 Rokushima and Yamakita Theory

It is a rigorous theory for anisotropic dielectric gratings of arbitrary shape. The beauty of the RY theory is that it can be applied to both Bragg and the phase grating modes. It has been discussed in detail in references [1] and [2]. Here we consider the RY theory applied to the phase grating mode. We consider Sc* phase with the twist axis along the Y direction and assume the medium to be infinite in extent in the XY plane and having a thickness d along the Z direction. Following the coupled wave analysis [1] we write the Maxwell's equations in the form

$$\frac{d\Psi(z)}{dz} = ik_0 \mathbf{D} \Psi(z) \quad (5.1)$$

where,

$$\Psi(z) = \begin{bmatrix} \mathbf{e}_x \\ \mathbf{h}_y \\ \mathbf{e}_y \\ \mathbf{h}_x \end{bmatrix}$$

$\mathbf{e}_x, \mathbf{e}_y, \mathbf{h}_y$, and \mathbf{h}_x are infinite sub-matrices of the infinite column matrix $\Psi(z)$ at any point z and contain the various Fourier components of the transverse electric and magnetic field. Also $k_0 = 2\pi/\lambda$, λ being the wavelength of the incident light. The propagation matrix \mathbf{D} which is a function of z is then given by the infinite square matrix

$$\mathbf{D} = \begin{bmatrix} 0 & I & 0 & 0 \\ \epsilon_{xx} - \epsilon_{xz}\epsilon_{zz}^{-1}\epsilon_{zx} - Q^2 & 0 & \epsilon_{xy} - \epsilon_{xz}\epsilon_{zz}^{-1}\epsilon_{zy} & -\epsilon_{xz}\epsilon_{zz}^{-1}Q \\ -Q\epsilon_{zz}^{-1}\epsilon_{zx} & 0 & -Q\epsilon_{zz}^{-1}\epsilon_{zy} & I - Q\epsilon_{zz}^{-1}Q \\ \epsilon_{yx} - \epsilon_{yz}\epsilon_{zz}^{-1}\epsilon_{zx} & 0 & \epsilon_{yy} - \epsilon_{yz}\epsilon_{zz}^{-1}\epsilon_{zy} & -\epsilon_{yz}\epsilon_{zz}^{-1}Q \end{bmatrix}$$

Here, ϵ_{xz} etc., are infinite square matrices containing the Fourier components of the elements of the dielectric tensor such that $(\epsilon_{xz})_{\ell j} = \epsilon_{xz(\ell-j)}$, Q are infinite

diagonal matrices with elements $q_0 + nq$ with n going from $-\infty$ to ∞ , q_0 is the incident wavevector in the bounding isotropic media, q is the grating wavevector and \mathbf{I} is an infinite unit matrix. From the modal analysis described by Galatola et. al. [2], the solution of equation (5.1) leads to

$$\Psi(d) = \exp(ik_0d\mathbf{D})\Psi(0) = U\Psi(0). \quad (5.2)$$

To compare the computations with experimental results it is convenient to write $\Psi(z)$ in terms of the modes in the bounding isotropic media. We assume the bounding region to have the refractive index equal to the mean refractive index of the Sc* medium. Then $\Psi(z)$ in these regions can be written as

$$\Psi(z) = \mathbf{T}\phi(z) \quad (5.3)$$

where, \mathbf{T} is the matrix having the elements $\mathbf{T}_{\ell j}$, which are the ℓ^{th} component of the j^{th} eigenvector of the bounding isotropic media and $\phi(z)$ is the column vector containing the strength of the different modes in the isotropic media arranged in the same order. In our case they are the forward and backward propagating TE and TM modes arranged in the following order

$$\phi(z) = \begin{bmatrix} \phi_f TE \\ \phi_f TM \\ \phi_b TE \\ \phi_b TM \end{bmatrix}$$

Then from equation (5.2) we get

$$\phi(d) = \mathbf{T}^{-1}U\mathbf{T}\phi(0) = S\phi(0) \quad (5.4)$$

The matrix \mathbf{S} is called the scattering matrix and contains the optical properties

of the grating which are obtainable from an experiment. The vector $\phi(0)$ is the sum of the reflected and incident components while $\phi(d)$ is the transmitted component. Thus we write

$$\phi(0) = \phi_r + \phi_i = \begin{bmatrix} \phi_i \text{ TE} \\ \phi_i \text{ TM} \\ \phi_r \text{ TE} \\ \phi_r \text{ TM} \end{bmatrix}$$

$$\phi(d) = \phi_t = \begin{bmatrix} \phi_t \text{ TE} \\ \phi_t \text{ TM} \\ 0 \\ 0 \end{bmatrix}$$

The equation (5.4) can be split into

$$\phi_r = \mathcal{R}\phi_i \quad , \quad \phi_t = \mathcal{T}\phi_i \quad (5.5)$$

where \mathcal{R} and \mathcal{T} are the reflection and transmission matrices respectively.

We use Berreman's model [3] to evaluate the dielectric tensor for Sc* phase. According to this model, the dielectric tensor is given as follows

$$\begin{aligned} \epsilon_{x,x} &= \epsilon_1 \cos^2 \alpha + \sin^2 \alpha (\epsilon_2 \sin^2 \theta + \epsilon_3 \cos^2 \theta), \\ \epsilon_{y,y} &= \epsilon_1 \sin^2 \theta + \epsilon_3 \cos^2 \theta, \\ \epsilon_{z,z} &= \epsilon_1 \sin^2 \alpha + \cos^2 \alpha (\epsilon_2 \sin^2 \theta + \epsilon_3 \cos^2 \theta), \\ \epsilon_{x,y} &= \frac{1}{2} (\epsilon_2 - \epsilon_3) \sin \mathbf{a} \sin 2\theta, \\ \epsilon_{y,z} &= \frac{1}{2} (\epsilon_2 - \epsilon_3) \cos \mathbf{a} \sin 2\theta, \\ \epsilon_{x,z} &= \frac{1}{2} (\epsilon_1 - (\epsilon_2 \sin^2 \theta + \epsilon_3 \cos^2 \theta)) \sin 2\alpha, \end{aligned}$$

Here ϵ_1, ϵ_2 and ϵ_3 are the principal values of the dielectric tensor, θ is the tilt angle of the Sc* phase and $a = 2\pi P/y$. In the calculations, in principle, one has to

consider infinite number of Fourier components of the dielectric tensor. However it was found that it is sufficient to retain the Fourier components only up to the fifth order. The Sc^* medium is locally biaxial but in our calculations we assume it to be locally uniaxial. In fact we find that biaxiality does not effect the main results. Using equation (5.5), we have computed the intensities of the diffraction orders for varying sample thickness and tilt angle using the material parameters of SCE6.

5.3 Results and discussion

The intensities of the first order diffraction in HH and HV geometries as a function of sample thickness are shown in figure 5.1a and those for VH and VV geometries in figure 5.1b. The diffracted light intensity exhibits oscillations with sample thickness. The oscillations have periods of different length scales. We can see that in general the intensity for the HH geometry is higher than in the HV geometry for thickness in the range 50 - 200 μm in conformity with the experiments. Similarly, the intensity in the VH geometry is more than that of VV geometry. Figures 5.2a and 5.2b show the intensity of the second order in HH, HV, VH and VV geometries as a function of sample thickness. It may be noticed that even here, in general, the diffracted intensity is more for the HH geometry than in the HV geometry. Also the intensity in VH geometry is in general more than that in the VV geometry. Thus in the range 50 - 200 μm the computed results are in qualitative agreement with the observed results.

However, the theoretical calculations are not in agreement with the results observed for the 23 μm sample in the first order diffraction at all temperatures. In the

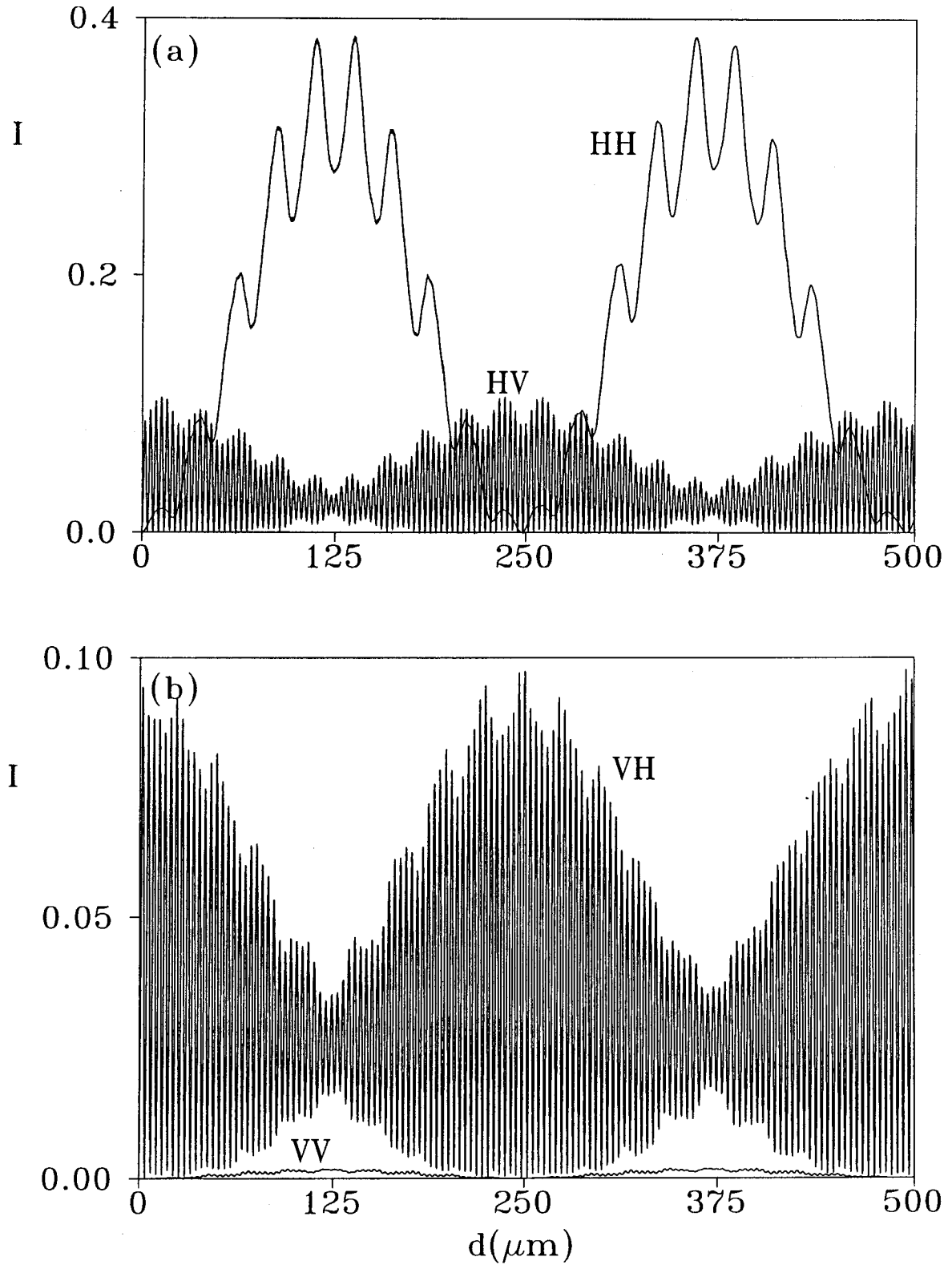


Figure 5.1: The computed normalized intensity I for the first order diffraction as a function of sample thickness (a) for the HH and HV geometries, (b) for the VH and the VV geometries. The parameters used in the calculation are; $P = 5\mu\text{m}$, $\Delta n = 0.18$ and $\theta = 18^\circ$.

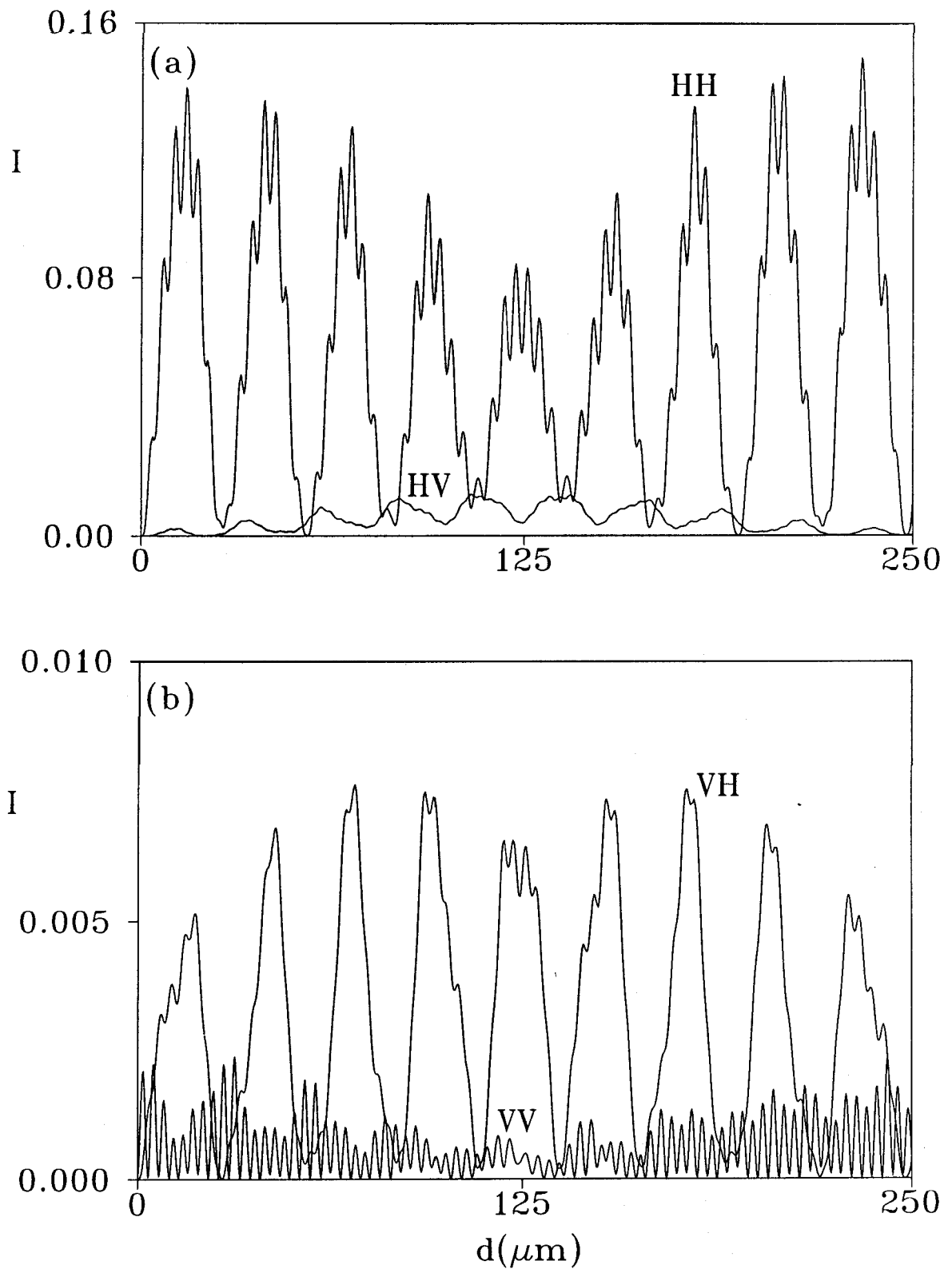


Figure 5.2: The computed normalised intensity I for the second order diffraction as a function of sample thickness for (a) HH and HV geometries and (b) for VH and VV geometries. The parameters used in the calculation are the same as those given in figure 5.1.

experiments we find that the intensities in the HH and VH geometries are always higher than that in the HV and VV geometries respectively as shown in figure 4.5a. The discrepancy in the 23 μm sample may be due to the deformation in the structure by the strong anchoring at the bounding surfaces. One has to incorporate the surface effects [4] appropriately to explain the observed effects in the 23 μm sample.

The computations show a reversal in the intensity between the HH and HV geometries around 250 μm as can be seen in figure 5.1a. This accounts for the observations at the high temperature ($T = 50.6\text{ }^\circ\text{C}$) for 250 μm sample. However, the computations carried out using the same parameters can not explain the observations at low temperature ($T = 45.5\text{ }^\circ\text{C}$). This can be understood by appealing to the temperature dependence of the pitch (figure 4.1), tilt angle, and birefringence. All these parameters drastically change the intensity and polarization features of the diffracted light. In figure 5.3 we have given the computed intensity, as a function of the tilt angle θ , in the first order diffraction for the HH and the HV geometries in the case of a 250 μm thick sample. It is interesting to note that one can get a cross over in the intensity between the HH and HV geometries by just varying the tilt angle of the Sc^* phase. One can interpret the observed reversal of the polarization features in the 250 μm sample at low temperatures as being due to change in the material parameters with temperature. For the VV and VH geometries, though, we find the reversal of polarization feature in the experiments, the variation of tilt angle with temperature alone cannot explain this reversal. All these results are in complete variance with those of the approximate theory [5] which is valid only for very thin samples. For the material parameters for SCE6 the RN theory is valid only for very thin sample thickness ($\approx 2\mu\text{m}$).

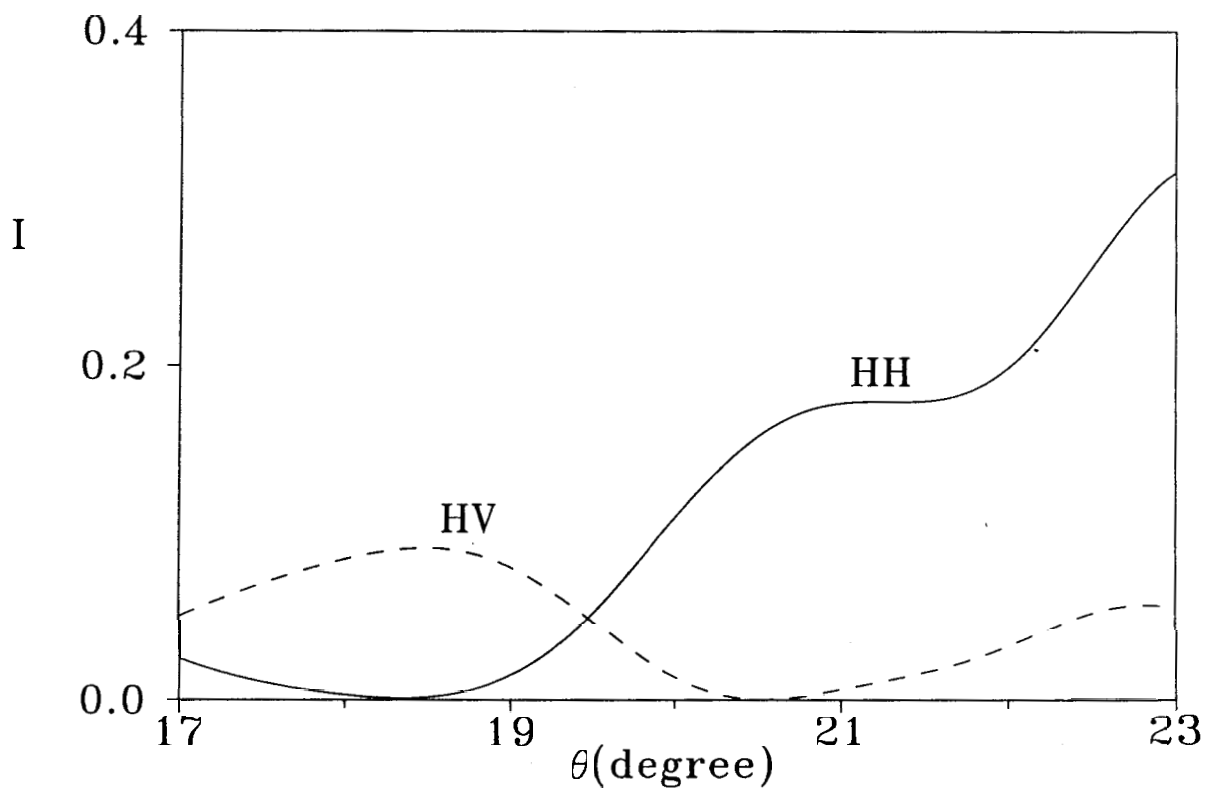


Figure 5.3: The computed normalized intensity I of the first order diffraction as a function of the tilt angle (θ) of the Sc^* phase for the HH and the HV geometries for $d=250\mu\text{m}$, $P = 5\text{pm}$ and $A_n = 0.18$

5.4 Remark on the oscillatory behaviour of the diffracted intensity

Another interesting feature in the computed results is the appearance of oscillations of different periods in the diffracted intensity as a function of sample thickness. For example in figure 5.1a for the HV geometry, the first order diffraction has fine fringes of width $4 \mu\text{m}$ which have another oscillation of period of about $25 \mu\text{m}$ superposed on it. For the IIH geometry the period of the oscillation is $250 \mu\text{m}$ with a smaller oscillation of period $25 \mu\text{m}$ superposed on it. Such oscillations of different periods are also present in the second order. Using a perturbation technique we show that these oscillations are the consequence of a coupling between different orders of scattering. In this section we discuss this perturbation technique. The technique is an alternate method to compute the diffracted intensity from the scattering matrix S . In this procedure we look at the propagation equation for the S matrix. To get this propagation equation, we start with equations (5.3) and (5.1) to get

$$\frac{d\phi(z)}{dz} = i k_o G(z)\phi(z) \quad (5.6)$$

where $\phi(z) = S\phi(0)$ and $G(z)$ is a new propagation matrix. Since \mathbf{T} matrix is independent of z , $G(z)$ is equal to $\mathbf{T}^{-1}\mathbf{D}\mathbf{T}$. From equation (5.6) we can write the propagation equation for the scattering matrix S as

$$\frac{dS}{dz} = i k_o G(z)S \quad (5.7)$$

The matrix $G(z)$ can be written as a sum of its z -independent diagonal matrix G_o corresponding to an effective homogeneous anisotropic medium and a small per-

turbative off-diagonal matrix g that contains the z dependence. It may be noticed that the above equation is analogous to the time dependent Schrodinger equation [6]. In this treatment $-i/\hbar$ is replaced by ik_o and the time evolution is analogous to the thickness variation of the grating in the z direction. This analogy allows us to use the well known time dependent perturbation theory of quantum mechanics [6] to study this problem.

The first, second and third order scattering contributions to the amplitude of the diffracted light, $(A_{S_I})_{\ell_j}$, $(A_{S_{II}})_{\ell_j}$ and $(A_{S_{III}})_{\ell_j}$, from the ℓ^{th} and the j^{th} scattered waves are given by

$$(A_{S_I})_{\ell_j} = ik_o \int_0^d dz \exp(ik_o E_j(d-z)) g_{\ell_j} \exp(ik_o E_\ell z) \quad (5.8)$$

$$(A_{S_{II}})_{\ell_j} = (ik_o)^2 \sum_k \int_0^d dz \int_0^z dz' (\exp(ik_o E_j(d-z)) g_{jk} \exp(ik_o E_k(z-z')) g_{k\ell} \exp(ik_o E_\ell z')) \quad (5.9)$$

$$(A_{S_{III}})_{\ell_j} = (ik_o)^3 \sum_k \sum_m \int_0^d dz \int_0^z dz' \int_0^{z'} dz'' (\exp(ik_o E_j(d-z)) g_{jk} \exp(ik_o E_k(z-z')) g_{km} \exp(ik_o(z'-z'')) g_{m\ell} \exp(ik_o E_\ell z'')) \quad (5.10)$$

The summations are over all the scattered waves. The element g_{ℓ_j} of the g matrix represents the coupling between the ℓ^{th} and the j^{th} order diffracted waves. E_ℓ and E_j are the eigenvalues of the corresponding waves in the effective homogeneous anisotropic medium.

We interpret these oscillations in the diffracted intensity as a function of sample thickness as follows. As stated earlier the propagation matrix $G(z)$ can be treated as the sum of two matrices viz, i) G_o that contains the diagonal terms

and ii) g that contains the off-diagonal terms. The matrix g can be treated as a perturbation over the matrix G_o . Equations (5.8), (5.9) and (5.10) give the first, second and third order scattering contributions to the amplitude of the diffracted wave for different polarizations. Figure 5.4a shows the first ($| (A_{S_I})_{HH} |^2$) and third ($| (A_{S_I})_{HH} + (A_{S_{II})_{HH}} + (A_{S_{III})_{HH}} |^2$) order perturbation contributions to the diffracted intensity in the first order diffraction for the HH geometry. Here one may note that the first order scattering contribution corresponds to the oscillations of $250 \mu\text{m}$ period and the third order perturbation has, in addition, the oscillation of $25 \mu\text{m}$ period seen in figure 5.1a for the HH geometry. Figure 5.4b shows the intensity contributions of different orders of perturbations to the first order diffraction for the HV geometry. We can see that the first order perturbation ($| (A_{S_I})_{HV} |^2$) only gives the fine oscillations of $4 \mu\text{m}$. The third order perturbation ($| (A_{S_I})_{HV} + (A_{S_{II})_{HV}} + (A_{S_{III})_{HV}} |^2$) gives this oscillation modulated with a larger period of $25 \mu\text{m}$. The contributions due to second order scattering is not very different from that of the first order. We would like to mention that the perturbation calculations are valid only for thin samples. However it gives a qualitative understanding of the oscillations in the diffracted intensity obtained from the rigorous theory.

In conclusion we see that the intensity and polarization features of the diffraction pattern in the phase grating mode of Sc^* is very sensitive to the sample thickness, birefringence, tilt angle and pitch of the medium. Many of the observed polarization features have been accounted for theoretically. The computed diffracted intensity as a function of sample thickness shows oscillations of different periodicities. These have been attributed to the interference effects from the different orders of scattering.

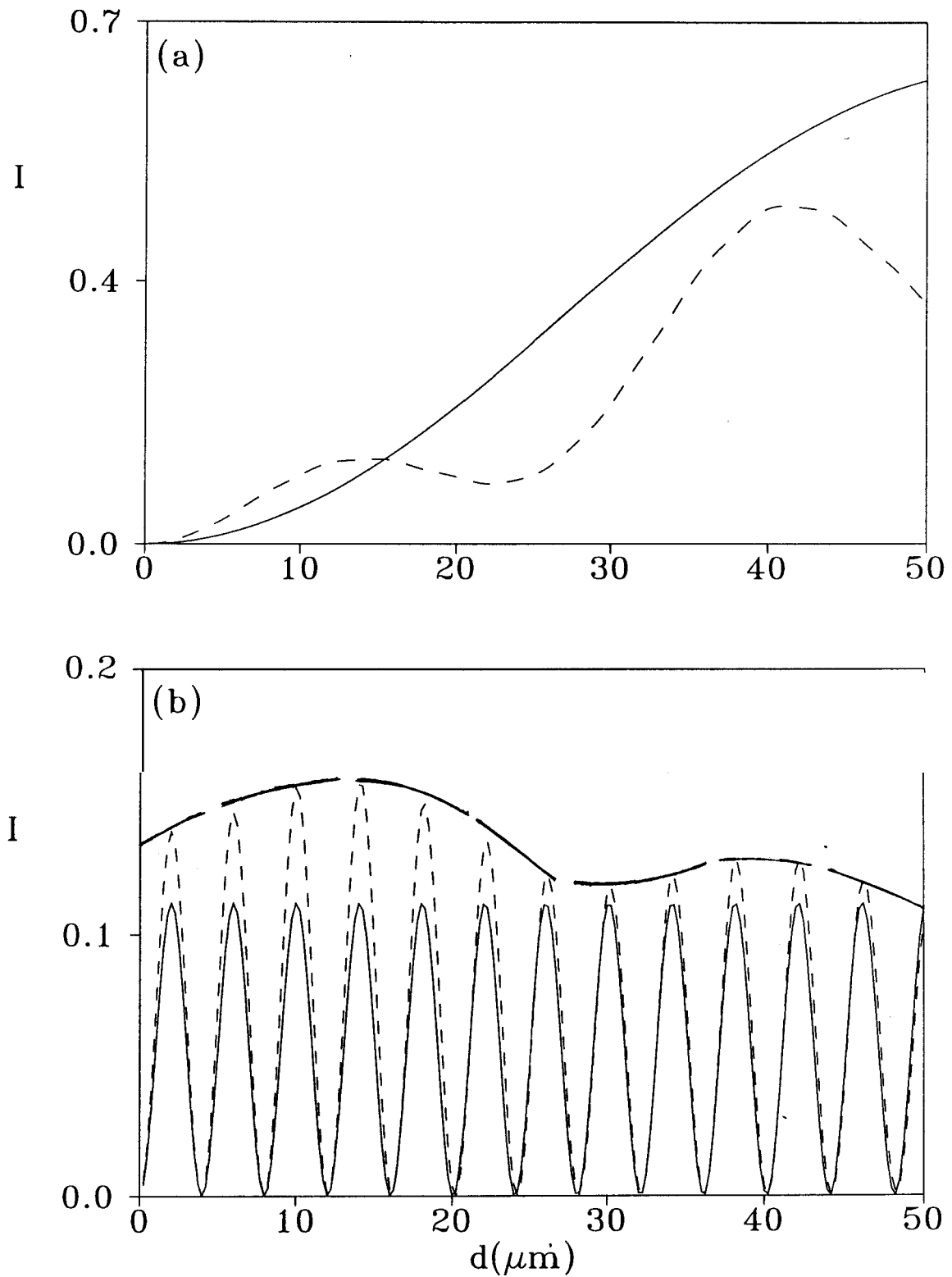


Figure 5.4: The normalized intensity I of the first order diffraction as a function of sample thickness computed using a perturbation theory (a) for the HH geometry, (b) for the HV geometry. The full line represents the contribution from the first order scattering and the dashed line represents third order scattering contribution to the diffracted intensity. In (b), a long dashed line is drawn over the peaks of the dashed curve as a guide to the eye to show the $25\mu\text{m}$ modulations.

References

- [1] K. Rokushima and J. Yamakita, "Analysis of anisotropic dielectric gratings", *J. Opt. Soc. Ame.*, 73, **901** (1983).
- [2] P. Galatola, C. Oldano and P.B. Sunil Kumar, "Symmetry properties of anisotropic dielectric gratings", *J. Opt. Soc. Ame. A*, **11**, 1332 (1994).
- [3] D. W. Berreman, "Twisted smectic C phase: unique optical properties", *Mol. Cryst. Liquid Cryst.*, 22, **175** (1973).
- [4] Povše T., Muševič I., Žekš B. and Blinc R., "Phase transition in ferroelectric liquid crystals in a restricted geometry", *Liq. Crystals*, 14, **1587** (1993).
- [5] K.A. Suresh, P.B. Sunil Kumar and G.S. Ranganath, "Optical diffraction in twisted liquid-crystalline media - phase grating mode ", *Liq. Crystals*, **11**, **73** (1992).
- [6] A. Messiah, *Quantum Mechanics volume(II)*, North Holland Publishing Company, Amsterdam, (1970).

Chapter 6

Optical diffraction in a quasi-periodic liquid crystalline medium

6.1 Introduction

In the previous chapters, we considered optics of periodic structures. Even systems which are quasi-periodic can exhibit very interesting optical properties. In this chapter we consider the optics of one such medium.

Since the discovery of quasi-periodic materials by Shechtman et.al.[1], the subject has attracted a lot of attention. The pioneering works of Levine and Steinhardt [2], and Socolar and Steinhardt [3] on quasi-periodic tilings have led to many new insights into the structure of such systems. In recent times quasi-periodic gratings and multilayers [4,5] have indeed been made in the laboratory [6,7]. This has led to the study of their optical properties. Self similarity in the reflection band [4], localization of light [4,7] and power law transmittance with a critical exponent [6] are some of the interesting features associated with such systems.

In this chapter we address ourselves to a quasi-periodic helical stack of birefringent layers such as cholesteric liquid crystals in both Bragg and phase grating modes. As stated earlier that it has been proposed that the Blue phase III can have quasi-periodic ordering [8,9]. A study of such a structure will give more insight for

the better understanding of the structure of BP III.

6.2 Structure of quasi-periodic lattices

We consider a quasi-periodic structure constructed according to a procedure due to Levine and Steinhardt [2]. The N^{th} lattice point of the quasi-periodic lattice is given by

$$X_N = (N + \tau + h[h N + \sigma]) l \quad (6.1)$$

where τ and a are arbitrary real numbers, h is an irrational number and N is an integer. Here $[]$ means that we take only the greatest integral value of the term inside the bracket. For $h = 0$ the structure becomes periodic with a spacing 1. For $1/h = (\sqrt{5} + 1)/2$ the difference $X_{N+1} - X_N$ will be one of the two incommensurate lengths l_1 and l_2 such that $l_2 = (h + 1) l_1$. The two lengths l_1 and l_2 occur according to the Fibonacci sequence (FS). For any other value of h we get an entirely different sequence. Changes in the value of τ results in the shift of the lattice. Different values of a generate different FSs and these sequences are locally isomorphic [2], i.e., arbitrarily large regions of the two sequences can be made identical.

The standard FS can also be generated using an iterative method [4]. The j^{th} sequence is given by

$$M_j = (M_{j-1}, M_{j-2}) \quad (6.2)$$

with $M_0 = (S_1)$ and $M_1 = (S_2)$ where S_1 and S_2 are the two distinct elements of the FS. For example $M_2 = (S_2, S_1)$, $M_3 = (S_2, S_1, S_2)$ and $M_4 = (S_2, S_1, S_2, S_2, S_1)$. It is worth mentioning here that in this procedure it is not possible to generate isomorphic FSs.

6.3 Diffraction in a quasi-periodic cholesteric

6.3.1 Bragg mode

Optical Bragg reflections from quasi-periodic multilayers [4,5,6] have been studied in systems with optically isotropic layers. We consider here a system with anisotropic layers. The quasi-periodic cholesteric liquid crystal could be a good example for such a system. We consider this structure to be made of two incommensurate but uniformly twisted regions of thicknesses l_1 and l_2 occurring in a FS. Within each such unit we have a uniform helical stack of birefringent layers as in cholesteric, with a total twist of 2π . Also $l_1 = (1 + h)l_2$. Here the dielectric tensor is locally uniaxial. The incident light enters the medium along the twist axis (normal incidence). The electromagnetic wave propagation in this medium can be analyzed using the 4 x 4 Berreman's matrix method described in chapter 2. According to this approach a column vector ψ is defined in terms of the electric and magnetic field components

$$\psi = \begin{bmatrix} E_x \\ H_y \\ E_y \\ -H_x \end{bmatrix}$$

In terms of ψ the Maxwell's equations can be written in the following matrix form

$$\frac{\partial \psi}{\partial z} = \frac{i\omega}{c} \Delta(z) \psi \quad (6.3)$$

where the matrix $\Delta(z)$ depends on the dielectric tensor. For the quasi-periodic structure we first compute the propagation matrices F and F for the two elements of incommensurate thicknesses l_1 and l_2 . The net propagation matrix F_j for the j^{th} Fibonacci sequence is obtained by multiplying sequentially F and F according to

the FS. For example for $j = 5$, $\mathbf{F}_j = \mathbf{F}'\mathbf{F}'\mathbf{F}'\mathbf{F}'\mathbf{F}'$.

If ψ_t , ψ_r and ψ_i are the transmitted, reflected and the incident fields then we have the relation

$$\psi_t = \mathbf{F}_j(\psi_i \mathbf{t} \psi_r) \quad (6.4)$$

Expressing the reflected and the transmitted fields in terms of the incident field one can calculate the reflectance and the transmittance of the quasi-periodic medium.

We assume a right handed quasi-periodic medium, with the local principal dielectric constants to be $\epsilon_1 = 2.14$ and $\epsilon_2 = 2.35$. We find that at normal incidence, the eigenwaves are to a good approximation, right and left circular waves, i.e., they are same as those for a normal cholesteric. The left circular wave always propagates without any attenuation but the right circular wave suffers attenuation, i.e., it gets Bragg reflected. The positions of the Bragg peaks are given by

$$\lambda_o = \frac{\bar{n} l (1 + h^2)}{(r + s h)} \quad (6.5)$$

where \bar{n} is the mean refractive index of the medium, l is the period of the medium when $h = 0$, r and s are integers. It is interesting to note that the position of the Bragg peak is dependent on two integers namely r and s . However, in the periodic structure of cholesteric only one Bragg peak occurs. This will be situated at $\lambda_o = \bar{n}l$.

Figures 6.1a and 6.1b show the reflection spectra for a quasi-periodic cholesteric with 10 and 25 elements respectively. As we increase the number of elements, the incident wave sees as it were more and more quasi-periodicity and as a result new reflection bands appear. This can also be seen from the dispersion curves shown in figures 6.2a and 6.2b for the same structures. One of the interesting properties

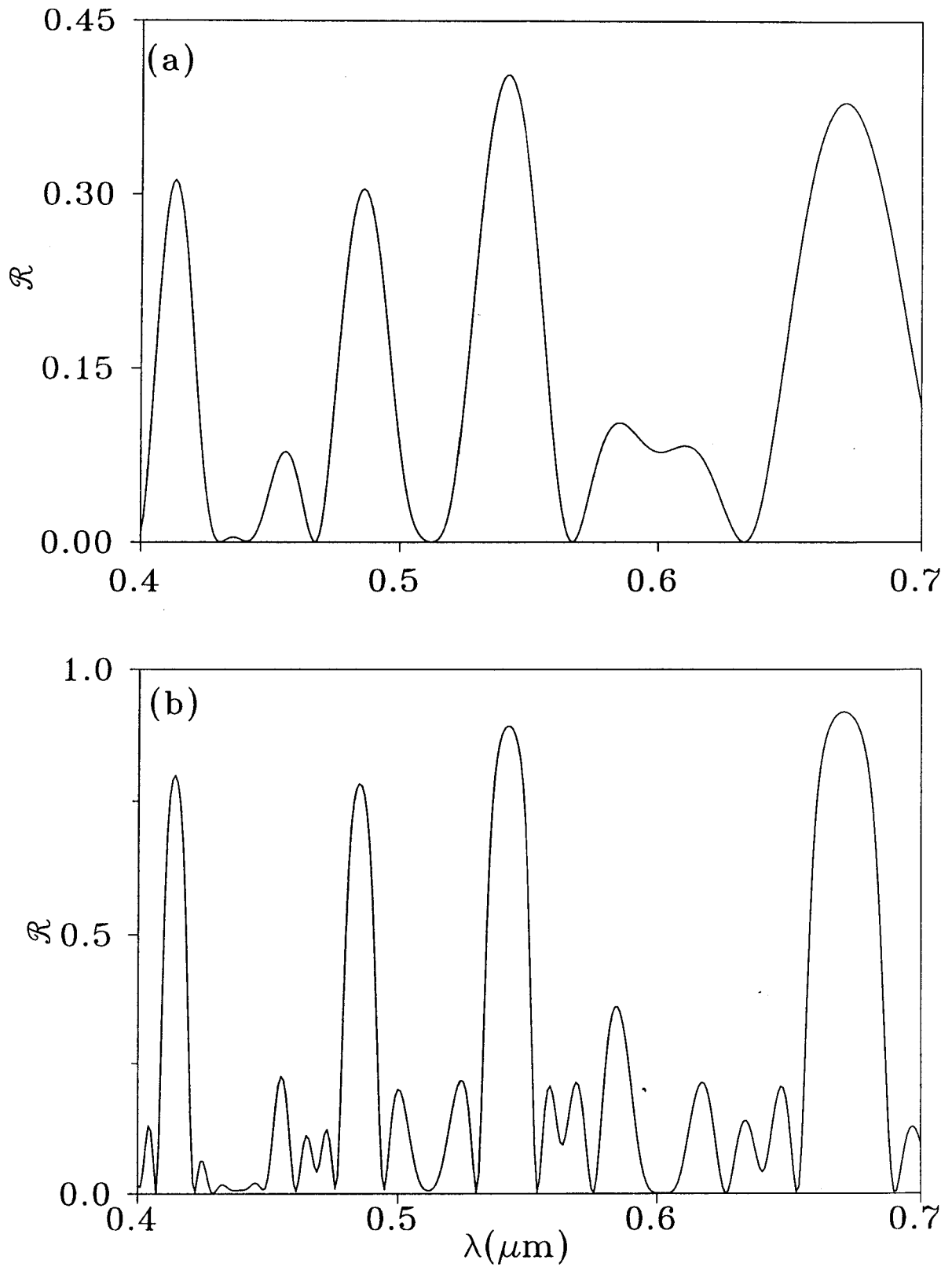


Figure 6.1: Reflection spectrum for a quasi-periodic cholesteric medium (a) 10 elements (b) 25 elements.

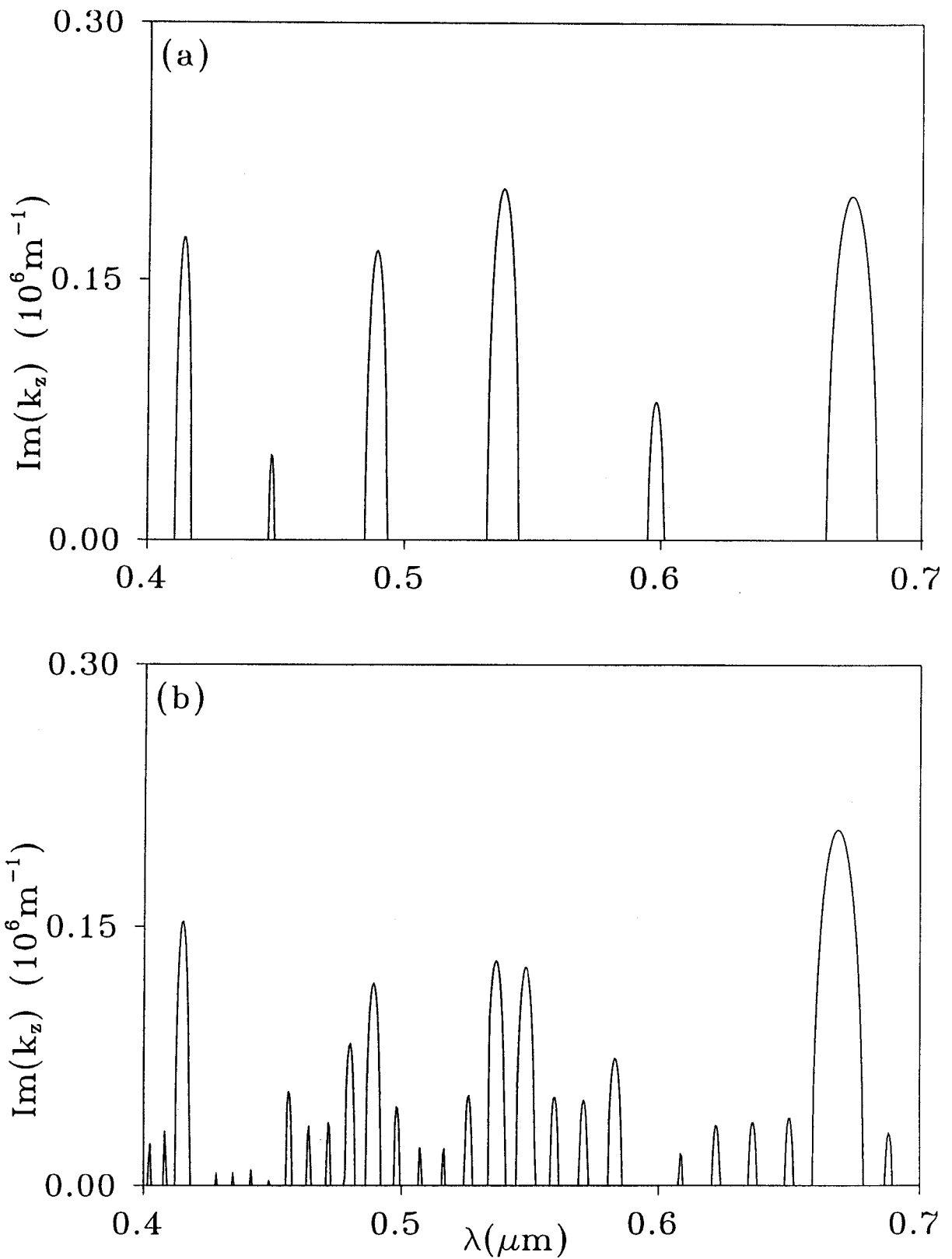


Figure 6.2: Dispersion curve for a quasi-periodic cholesteric medium (a) 10 elements, (b) 25 elements. Here k_z is the wavevector inside the medium.

associated with this medium is the self-similarity of the reflection spectra [4,5,7]. This self-similarity is a consequence of a six-cycle mapping for the propagation matrix, i.e., $\mathbf{F}_j = \mathbf{F}_{j+6}$. We have compared the reflection spectra obtained for 55 elements for the region $\lambda = 0.47\mu\text{m}$ to $0.56\mu\text{m}$ (fig. 6.3a) with that of 233 elements (fig 6.3b) for the region $\lambda = 0.5\mu\text{m}$ to $0.525\mu\text{m}$. We can clearly see that in this case there is a self-similarity between the two reflection spectra.

We have also worked out the nature of the standing waves in the Bragg bands. As in normal cholesterics here also the net E field of the standing wave is a linear vibration, with $\mathbf{E} \parallel \mathbf{H}$ [11]. The azimuth of the E field rotates by $\pi/2$ as we move from one edge of any reflection band to its other edge. In a given reflection band the azimuth of the E field uniformly rotates as we move along the twist axis, with a constant period. This period is different in different reflection bands. Also the intensity of the E field for the non-propagating mode gets attenuated by different amounts in different reflection bands, but in every band the decay is non exponential. This is in contrast to the exponential decay found in normal cholesterics [12,13].

The effect of dichroism can be easily worked out. In figure 6.4 we have given the reflection spectra for 25 linearly dichroic birefringent elements. Comparing this with the reflection curve shown in figure 6.1b, for an identical non-absorbing sequence, it can be noticed that many of the reflections of the non-absorbing multilayer stack are absent in the absorbing case. This is due to the fact that the incident wave gets more attenuated inside the medium because of absorption before it can experience the quasi-periodic nature of the lattice.

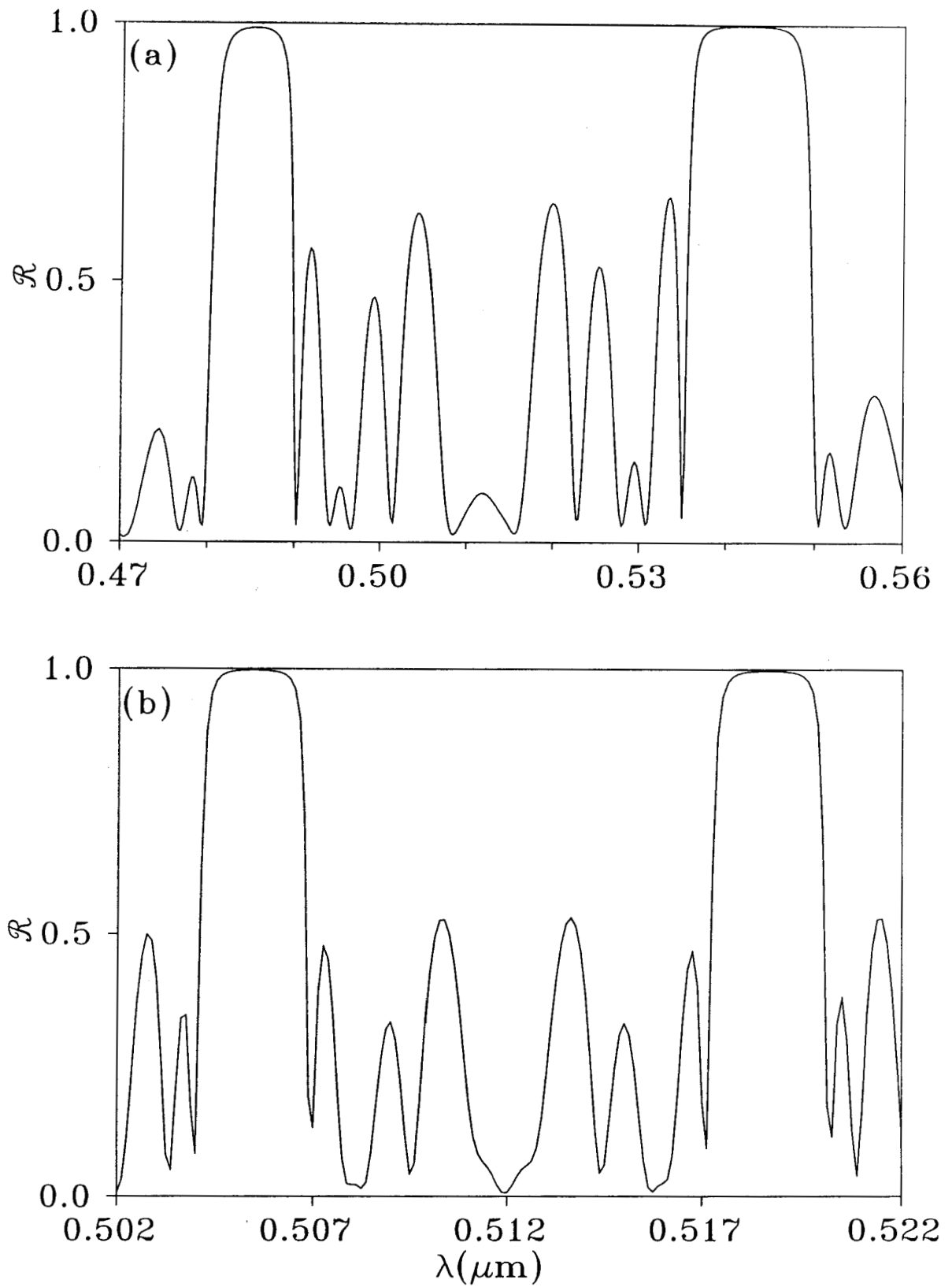


Figure 6.3: The reflection spectrum of (a) 55 and (b) 233 elements in the quasi-periodic cholesteric medium. By comparing (a) and (b) one may note the self-similarity between the two spectra.

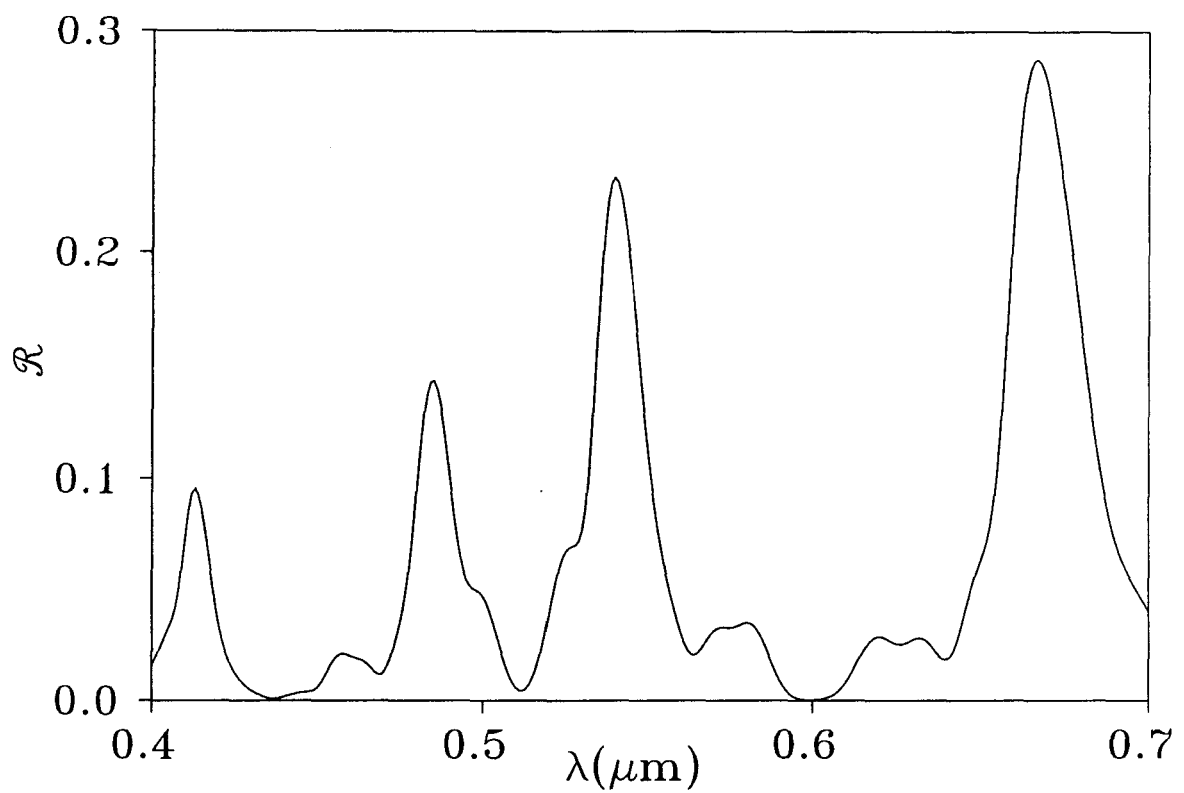


Figure 6.4: Reflection spectrum for an absorbing 25 elements thick quasi-periodic cholesteric medium. Here $\text{Im}(\epsilon_1) = 0.0063$ and $\text{Im}(\epsilon_2) = 0.063$. This may be compared with figure (6.1b) which represents the reflection spectrum for an identical multilayer without absorption.

6.3.2 Phase grating mode

We now consider phase grating effects that can appear in such a quasi-periodic structure. Mosseri and Bailly [14] considered theoretically RN diffraction from a quasi-periodic structure obtained by superposing two ultrasonic waves of incommensurate wavelengths. This has many peculiar features not found in the classical periodic phase gratings. Recently RN diffraction from a fivefold quasi-periodic structure obtained by superposing five ultrasonic waves in a liquid has also been studied experimentally [15].

Here we study the phase grating effect in a locally anisotropic quasi-periodic structure. We assume the incident plane wavefront to be linearly polarized with its azimuth perpendicular to the twist axis and it is falling normal to the twist axis of the medium. The refractive index for this polarization varies along the twist axis. At any point the refractive index n_z for this polarization is given by

$$\frac{1}{n_z^2} = \frac{\cos^2(\vartheta)}{n_1^2} + \frac{\sin^2(\vartheta)}{n_2^2} \quad (6.6)$$

where ϑ is the azimuth of the major axis of the local index ellipsoid whose principal refractive indices are n_1, n_2 . Then the emergent wavefront is quasi-periodically corrugated. This leads to optical diffraction. We have shown in figure 6.5 the computed diffraction pattern using RN theory. It was mentioned earlier that in a periodic cholesteric in the same geometry the diffraction peaks will occur for the wavevectors $q = 2\pi(N/l)$ where l is the pitch of the periodic structure. However, the diffraction pattern of a quasi-periodic medium [2,3] has peaks at q

$$q = \frac{2\pi}{l(1+h^2)}(r + hs) \quad (6.7)$$

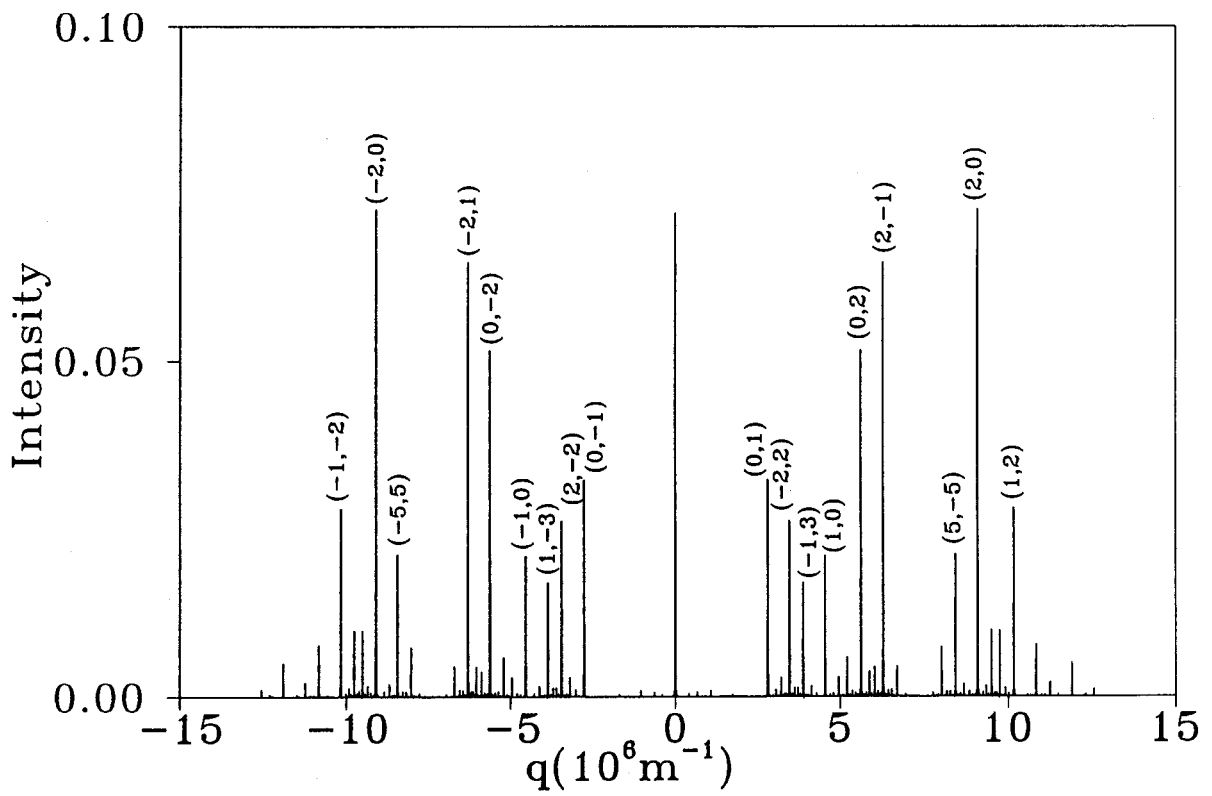


Figure 6.5: Diffraction pattern for a quasi-periodic cholesteric medium in the phase grating mode for $n_1 = 1.535$, $n_2 = 1.565$, sample thickness = $20 \mu\text{m}$, $\lambda = 0.633 \mu\text{m}$ and $l = 0.2618 \mu\text{m}$. We have given the pairs of integers (r, s) only for the intense peaks.

It is well known that in a quasi-periodic amplitude grating the intense diffraction peaks occur when r and s are in the ratio of successive Fibonacci numbers [2]. But interestingly in a quasi-periodic phase grating we do not find this result. The intensity in any given order is a function of the birefringence of the medium, sample thickness and wavelength.

It was mentioned in chapter 2 that linear dichroism can be introduced into the system by doping it with solute molecules. Then, generally, the local solute concentration depends on the local twist of the medium and to a good approximation it is inversely proportional to the twist in the medium. This leads to a non-uniform absorption in the quasi-periodic cholesteric. In such a non-uniformly absorbing system we get diffraction even for an incident light linearly polarized parallel to the twist axis. This is due to the variations in the magnitude of the amplitude of the emergent wavefront. It is important to note that diffraction in this geometry will be totally absent in a uniformly absorbing periodic or quasi-periodic cholesteric medium.

6.3.3 Effect of the variable a on diffraction

We have already shown in equation (6.1) that a change in a leads to an isomorphic FS. In both the amplitude and phase gratings (see Appendix B) the diffraction pattern obtained for different FSs that are isomorphic have peaks at same positions but the phases of the corresponding orders are different. This phase is a function of a . However in the case of a multilayered medium in the Bragg reflection mode which incorporates multiple reflections, we get a very interesting result. The intensity of

some of the Bragg reflections get altered as a changes. This is shown in figure 6.6 for a particular Bragg reflection.

In conclusion we have theoretically investigated the optical diffraction in a quasi-periodic cholesteric medium. In the Bragg mode we find that the quasi-periodicity of the medium gives rise to many reflection bands even at normal incidence. The number of band increases with the quasi-periodicity. The presence of absorption suppresses many of the reflection bands. In the phase grating mode the intense diffraction peaks can be indexed by a pair of integers. But the integers need not be in the ratio of successive Fibonacci numbers. The isomorphic FS gives same diffraction patterns in the phase grating mode but in the Bragg mode, they have different reflection spectra.

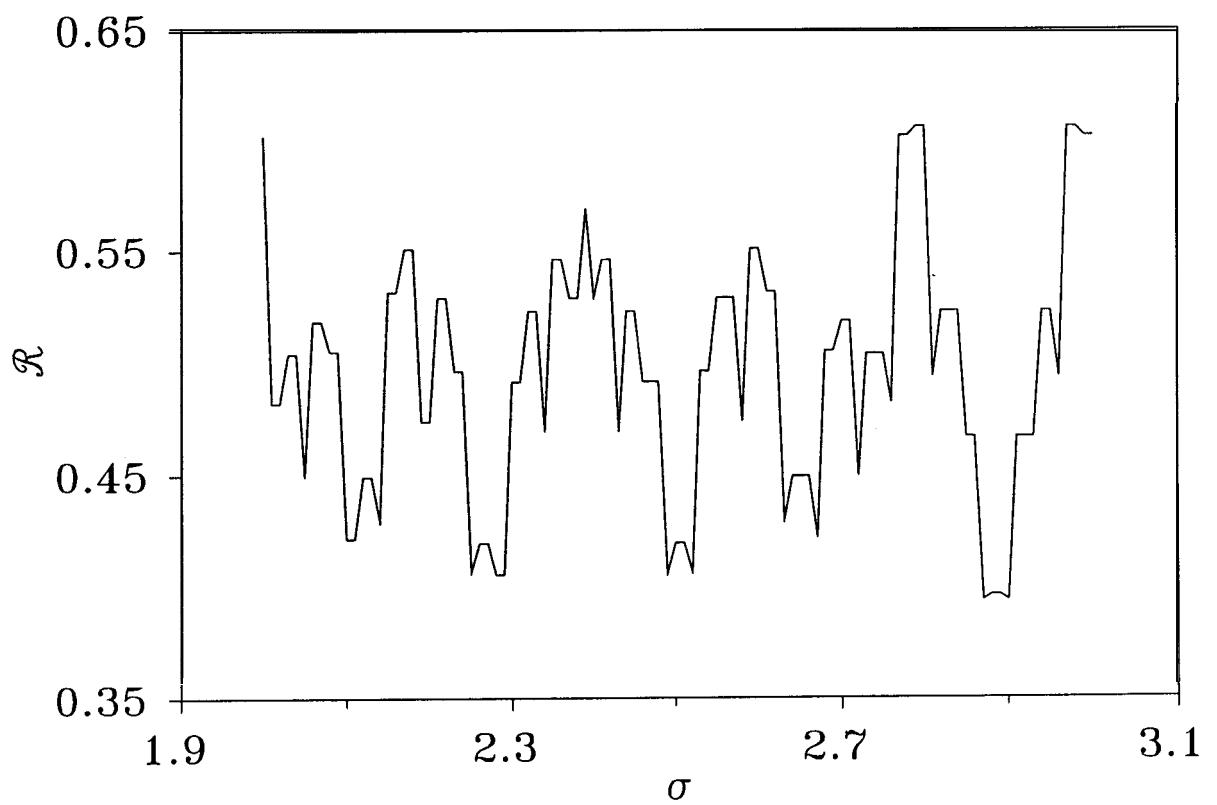


Figure 6.6: Intensity of Bragg reflection at $\lambda = 0.505 \mu\text{m}$ as a function of σ for **233** elements.

References

- [1] D. Shechtman, I. Blech, D. Gratias and J.W. Cahn, "Metallic phase with long-range orientational order and no translational symmetry", *Phys. Rev. Letts.*, **53**, 1951 (1984).
- [2] D. Levine and P. J. Steinhardt, "Quasicrystals I. Definition and structure.", *Phys. Rev. B*, **34**, 596 (1986).
- [3] J. E. S. Socolar and P. J. Steinhardt, "*Quasicrystal II*. Unit cell configuration", *Phys. Rev. B*, **34**, 617 (1986).
- [4] M. Kohmoto, B. Sutherland and K. Iguchi, "Localization in optics: *Quasiperiodic media*", *Phys. Rev. Letts.*, **58**, 2436(1987).
- [5] A. Latgé and F. Claro, "Optical propagation in multilayered system", *Optics Communications*, **94**, 389 (1992).
- [6] L. Chow and K. H. Guenther, "Critical field pattern in optical Fibonacci *multilayered system*", *J. Opt. Soc. Ame. A*, **10**, 2231 (1993).
- [7] W. Gellermann, M. Kohmoto, B. Sutherland and P.C. Taylor, "Localization of light waves in fibonacci dielectric *multilayer*", *Phys. Rev. Letts.*, **72**, 633 (1994).

- [8] **Il. M. Hornreich and S. Shtrikman**, "A *quasicrystalline structure for the cholesteric Fog phase* ", Phys. Letts. A, 115, **451 (1986)**.
- [9] **D. S. Rokhsar and J. P. Sethna**, "Quasicrystalline texture of *cholesteric liquid crystals: Blue phase III* ", Phys. Rev. Letts., 56, **1727 (1986)**.
- [10] **D.W. Berreman**, "Optics in stratified and anisotropic medium: *4 x 4- matrix formulation*", J. Opt. Soc. Ame., 62, **502 (1972)**.
- [11] **H. Zaghoul and H.A. Buckmaster**, "Transverse electromagnetic standing waves with $E \parallel B$ ", Am. J. Phys., 56, **801 (1988)**. **Hans De Raedt, Ad Lagendijk and Pedro de Vries**, "Transverse localization of light", Phys. Rev. Letts., 62, **47 (1989)**.
- [12] **P.B. Sunil Kumar and G.S. Ranganath**, "*Structural and optical behavior of cholesteric soliton lattices*", J. Phys. II France, 3, **1497 (1993)**.
- [13] **Yuvaraj Sah and K.A. Suresh**, "Anomalous transmission in absorbing *cholesterics* at oblique incidence ", J. Opt. Soc. Ame. A, 11, **740 (1994)**.
- [14] **R. Mosseri and F. Bailly**, "The diffraction of light by quasiperiodic ultrasound ", J. Phys. I France, 2, **1715 (1992)**.
- [15] **F. M. de Espinosa, M. Torres, G. Pastor, M. A. Muriel and A. L. Mackay**, "Acoustic quasicrystals", Europhys. Lett., 21, **915 (1993)**.